ELSEVIER

Biochimica et Biophysica Acta 1327 (1997) 52–60

BIOCHIMICA ET BIOPHYSICA ACTA
BBA

A calcium-activated, large conductance and non-selective cation channel in *Paramecium* cell

Fumihito Saitow [a,b], Yasuo Nakaoka [b], Yoshio Oosawa [a,*]

[a] *International Institute for Advanced Research, Matsushita Electric Industrial Co., Ltd., 3-4 Hikaridai, Seika, Kyoto 619-02, Japan*
[b] *Department of Biophysical Engineering, Faculty of Engineering Science, Osaka University, Toyonaka, Osaka 560, Japan*

Received 2 January 1997; revised 11 February 1997; accepted 20 February 1997

Abstract

A non-selective cation channel was found in mutant *Paramecium* cells (K115). This cell had been selected as a resistant mutant in a high-K^+ solution. In patch clamp studies of these cells in the inside-out configuration, this channel was activated by bath applications of elevated Ca^{2+} concentrations. The channels became very active when the Ca^{2+} concentration was above 3.2 μM. The channel was also activated by depolarization. The voltage dependency was steep upon depolarization, whereas upon hyperpolarization the channel activity barely changed. This channel had poor selectivity for monovalent alkali cations. Using the Goldman–Hodgkin–Katz equation for the reversal potential, the permeability ratios with respect to K^+ for Na^+, Rb^+, Cs^+ and Li^+ were nearly 1. Although the permeability ratios were similar for each cation, the single channel conductances differed. The single channel conductances were 467 pS with K^+ as the charge carrier, 406 pS with Na^+, 397 pS with Rb^+, 253 pS with Cs^+ and 198 pS with Li^+ upon depolarization in 100 mM cation solutions. A similar calcium-activated large conductance channel was observed in the wild-type (G3) *Paramecium* cells but was very rare. © 1997 Elsevier Science B.V.

Keywords: Channel; Calcium-activated channel; Non-selective cation channel; Cation channel; Patch clamp; (*Paramecium*)

1. Introduction

Extensive electrophysiological study of *Paramecium* cells has been carried out, and various types of channels were revealed [1,2]. To date, not only macroscopic currents but also single channel currents were recorded from planar lipid bilayers [3], patches excised from surface blisters [4] and reconstituted artificial liposomes [5]. Modulation of the free intracellular Ca^{2+} concentration is obviously essential in signal transduction and cell function. In *Paramecium* cells, several Ca^{2+}-dependent channels were reported by use of a patch clamp technique. These channels include two types of K^+-selective channels [2,4] and also Ca^{2+}-calmodulin activated Na^+ channels [6].

We reported that in the presence of methylene blue as a photosensitizer, light-spot stimulation to an anterior and a posterior part of the *Paramecium* cell induced a depolarization and a hyperpolarization of the membrane, respectively [7]. Under the voltage clamp condition, the anterior stimulation induced an inward Ca^{2+} current, while the posterior stimulation induced primarily a K^+ outward current. We concluded that the photodynamic action of methylene

* Corresponding author. Fax: +81 774 982575. E-mail: yoshio@crl.mei.co.jp

PII S0005-2736(97)00044-8

blue primarily opened Ca^{2+} channels, and that the following influx of Ca^{2+} activated Ca^{2+}-dependent K^+ channels that were localized mainly on the posterior part of the membrane [7]. More recently, we found that mutant (K115) *Paramecium* cells showed a weak Ca^{2+}-dependent K^+ current produced by photodynamic stimulation (unpublished data). We attempted to determine the differences between the properties of the Ca^{2+}-dependent cation channels of the mutant and the wild-type *Paramecium* cells. We have found two types of Ca^{2+}-dependent cation channels from wild-type and the mutant *Paramecium* cells. We speculated that one of the channels was the Ca^{2+}-dependent K^+ channel that was previously reported [4], judging from the values of single channel conductances, Ca^{2+} dependency and voltage dependency of the channel. The channel properties in the wild-type and mutant cells were similar. The other channel was a large conductance, non-selective cation channel that was activated by intracellular free Ca^{2+}. This channel was rarely observed in the wild-type cell membrane but was seen very often in the mutant cell membrane. Although this channel has not been reported in *Paramecium*, non-selective cation channels have been found in various cells [8–12]. These channels may have a variety of roles, based on the properties of cation selectivities and conductances with permeant ions in each cell. In this report, we present the properties of the Ca^{2+}-dependent non-selective cation channel of the mutant (K115) *Paramecium* cell. This channel was effectively blocked by 1 mM Ba^{2+} from the intracellular side.

2. Materials and methods

2.1. Cells

Paramecium caudatum (K115, provided by Drs. M. Endoh and M. Takahashi, Tsukuba, Japan) was used. This cell was selected as a resistant mutant in a high-K^+ solution. Cells were grown at 31°C in casamino acids media, similar in composition to previously described media [4]. The media contained 0.3 g/l casamino acids, 4 mM KCl, 0.44 mM Na citrate, 0.1 mM $CaCl_2$, 0.08 mM $MgCl_2$, 5 mg/l stigmasterol, 7.5 mg/l phenol red, and 5 mM *N*-2-hydroxyethylpiperazine-*N*′-2-ethanesulfonic acid (Hepes), adjusted to pH 7.0 with tris(hydroxymethyl)aminomethane (Tris) base. The culture media were bacterized with *Klebsiella pneumoniae* and inoculated with paramecia for 3–4 days. Bacteria were added again the day before the experiment to keep the paramecia in log-phase growth.

2.2. Isolation of plasma membrane

We employed a method of inducing blisters [4] because it was difficult to patch clamp an intact or live cells. Cells were withdrawn from the culture and put in a blister-inducing solution composed of 60–80 mM Na glutamate, 10^{-5} M free Ca^{2+} (buffered with 1 mM ethylene glycol bis(β-aminoethyl ether)-*N*,*N*,*N*′,*N*′-tetraacetic acid (EGTA)), 5 mM Hepes, 0.01 mM ethylenediaminetetraacetic acid (EDTA) and 1 mg/ml leupeptin. This solution was similar to that described [4] except for the concentration of Na glutamate, since solution with 100–150 mM Na glutamate could not induce the blisters adequately. Within 30 min the cells were covered with blisters of about 20 μm in diameter. These blisters were stripped from the body by forcing the cell through a glass micropipette. The isolated membrane vesicles derived from the blisters were transferred to another chamber filled with experimental solution (described below) of which the concentration of free Ca^{2+} was 10^{-8} M to form the gigaohm seal. Most membrane vesicles apparently consisted of an inner and an outer membrane, presumably with the plasma membrane outside. From the inner membrane any channel activity was not detected and the inner membrane might be the alveolar membrane [4]. The outer membrane was used for forming the gigaohm seal.

2.3. Electrophysiological measurements

The composition of solutions was the same as that previously described [4]. The experimental solutions were composed of the following basic ingredients unless stated otherwise: 100 mM K^+, 10^{-4} to 10^{-8} M free Ca^{2+}, 5 mM Hepes, 0.01 mM EDTA with 20 mM Cl^- and approximately 80 mM glutamate at pH 7.0 adjusted with L-glutamic acid (100 mM K^+ standard solution). Free Ca^{2+} was buffered with 1 mM EGTA. 50, 828, 941 or 979 μM total Ca^{2+} was added and buffered with 1 mM EGTA to give a final

free Ca^{2+} concentration of 10^{-8}, 10^{-6}, $3.2 \cdot 10^{-6}$ or 10^{-5} M, respectively [4]. The solution with 10^{-4} M Ca^{2+} contained no EGTA. All bath solutions contained 1 mM dithiothreitol to avoid possible oxidation. The patch clamp pipettes (Sutter Instrument, Novato, CA) were filled with 100 mM K^+ standard solution containing 10^{-8} M Ca^{2+}, and had resistances of 15–25 MΩ. For experiments to determine the ion selectivity of the channel, both the bath and the pipette were filled exactly the same solution containing 100 mM K^+ and 10^{-5} M Ca^{2+}. Under this condition, the potential of the membrane patch was corrected to null membrane current, and was defined as the zero potential of the membrane patch. The positioning of the reference electrode was done in two ways. (1) The reference Ag-AgCl electrode was directly immersed in the bath. (2) The reference Ag-AgCl electrode was encased in a glass capillary filled with 3 M KCl. This capillary was plugged with agar at the other end and immersed in the bath. There was no difference between the two ways. The seal resistances were greater than 5 GΩ. After the formation of the gigaohm seal, the patch membrane was excised by air exposure, achieving the inside-out excised patch clamp mode. When channel activity was observed, the patch was then exposed to a bath solution containing a higher Ca^{2+} concentration to examine the Ca^{2+} dependency of the channel. Since channel activity might decline rapidly like the Ca^{2+}-dependent K^+ channel in prolonged exposure to high-concentration Ca^{2+} ($> 10^{-6}$ M) [4], the patch was quickly moved back to the low-Ca^{2+} solution (10^{-8} M). In order to minimize these effects of Ca^{2+}, a quick perfusion system was devised for the analysis of Ca^{2+} dependency. Our system required about 2 s for solution exchange.

An Axopatch 200A amplifier (Axon Instruments, Foster City, CA) was used for single channel recordings. The single channel currents were filtered at 5 kHz through a 4-pole Bessel filter. An IBM PC/AT computer and pCLAMP software (Axon Instruments) were used for voltage ramp stimuli.

2.4. Data acquisition and analysis

Data were stored on a videotape recorder after digitizing by a digital data recorder (VR-100A, Instrutech, Elmont, NY). Single channel currents were digitized (sampling rate 2 kHz) after being filtered at 1 kHz using an 8-pole Bessel filter (model 902, Frequency Devices, Haverhill, MA) and analyzed using a program based on the pCLAMP6 software. Channel activity is expressed as NP_o, i.e., the integral of a current during a certain time period divided by the single channel current amplitude. Permeability ratios were calculated using the Goldman–Hodgkin–Katz equation,

$$I = \frac{z^2 P F^2 V}{RT} \left(\frac{[X]_i - [X]_o \exp(-zFV/RT)}{1 - \exp(-zFV/RT)} \right) \quad (1)$$

The subscripts ‘i’ and ‘o’ denote internal and external ion species, respectively. P is the permeability of the ion, V is the membrane potential, z is the valency of the ion, and F, R and T have their usual meanings. The current carried by each ion was calculated from Eq. (1).

All experiments were done at room temperature (21–23°C).

3. Results

Excised membrane patches from *Paramecium* contained a variety of ion channels. When K^+ was the major cation in both the pipette solution and the bath solution, two types of Ca^{2+}-dependent channels were encountered in most cases. One was a Ca^{2+}-dependent K^+ channel that was activated by hyperpolarization and had a conductance of about 70 pS in 100 mM K^+ (data not shown). We suspected that this channel was the Ca^{2+}-dependent K^+ channel previously reported [4]. The other type of channel had a large channel conductance and was activated by depolarization. The large conductance channels were encountered in more than 30% of the patches examined. Excluding empty patches, the number of current steps was 1.8 ± 0.75 (mean $\pm$ S.D.; $n = 35$) with 10^{-4} M Ca^{2+} solution.

3.1. Single channel conductance and ion selectivity of the large conductance channel

Fig. 1A shows typical current traces of the large conductance channels at various voltages in the presence of 100 mM K^+ with 10^{-5} M Ca^{2+}. The cur-

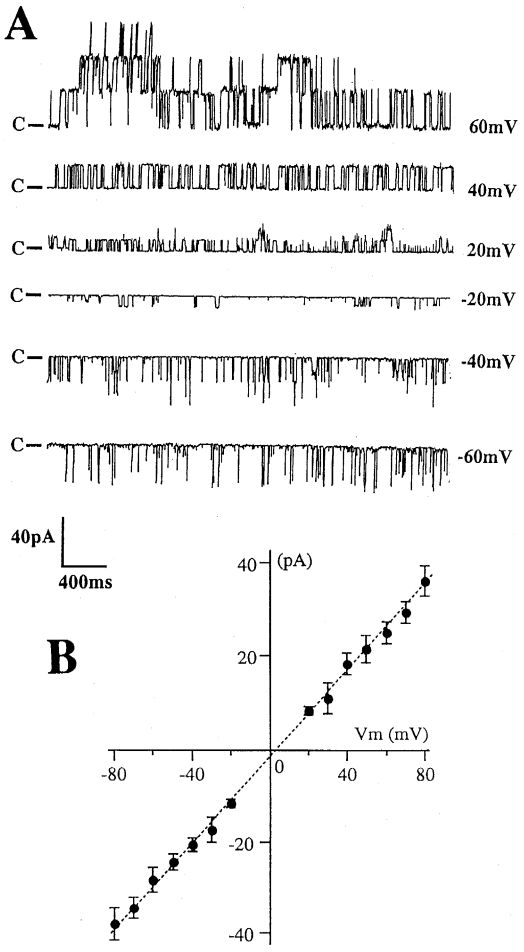

Fig. 1. Single channel currents and the current–voltage relationship for the large conductance channel. (A) Current records of a patch containing the large conductance channel in symmetrical 100 mM K^+ solution with 10^{-5} M Ca^{2+} at six membrane voltages. 'C' indicates closed level. (B) Current–voltage relationship for the large conductance channel in the inside-out configuration. Circles represent single channel currents (mean ± S.D.) from six patches for the symmetrical K^+ solution (100 mM K^+ in both pipette and bath) with 10^{-5} M Ca^{2+}. The dashed line indicates the result of a linear regression. The slope conductance was 462 pS.

rent–voltage relation of this channel was linear over the tested range, and thus the channel did not rectify (Fig. 1B). In the presence of 100 mM K^+ with 20 mM Cl^- and ~80 mM glutamate$^-$, the single channel conductance defined from the slope of the *I–V* curve was 462 pS (Fig. 1B). The ion selectivity of the channel was determined by replacing the bath solution. The composition of the solutions used for the ion selectivity experiments is shown in Table 1. Voltage ramp experiments were employed for determination of the reversal potential [13]. Similar values of the reversal potential were obtained from general voltage–current relationships. The applied voltage was changed linearly (0.160 mV/ms) from +100 to −100 mV (Fig. 2, top). Fig. 2 (middle) shows the voltage ramp induced currents when both the pipette solution and the bath solution were filled with 100 mM KCl. The crossing point that denotes the reversal potential was near 0 mV under the symmetrical condition. When the bath was perfused with 20 mM KCl solution (an other cation was not added), the reversal potential shifted to +35 mV (Fig. 2, bottom), which suggested a Cl^- to K^+ permeability ratio of 0.0685, according to the Goldman–Hodgkin–Katz equation for this asymmetrical condition. Further examinations were carried out using different cations in the bath and 100 mM K^+ standard solution in the pipette (Table 1). The permeability ratios with respect to K^+ for Na^+, Rb^+, Cs^+ and Li^+ were nearly 1. This channel may be described as a non-selective cation channel.

Fig. 3 shows the current–voltage relationship of the channel in the positive membrane potentials. The conductances were determined from the slope of the current–voltage relationships from experiments with 100 mM K^+ in the pipette and 100 mM of the respective cation in the bath. The tested cation passed through the membrane from the intracellular (bath) side to the extracellular (pipette) side in the positive membrane potentials. We considered that the conductances determined by the data obtained in the positive membrane potentials were the conductances of each cation in the bath side. In the voltage range tested, the conductances were 467 ± 8.2 pS for K^+ ($n = 6$), 406 ± 4.8 pS for Rb^+ ($n = 5$), 397 ± 9.0 pS for Na^+ ($n = 5$), 253 ± 8.3 pS for Cs^+ ($n = 5$) and 198 ± 5.6 pS for Li^+ ($n = 5$). Thus, the following conductance sequence for this channel was obtained.

$$g_K > g_{Rb} = g_{Na} > g_{Cs} > g_{Li}$$

3.2. Ca^{2+} dependency of channel activity

Fig. 4 shows the channel activity with different Ca^{2+} concentrations in the bath solution at +50 mV. When the channels were exposed to a high Ca^{2+} (10^{-4}–10^{-5} M) solution, the activation of the chan-

Table 1
Permeability ratios obtained by voltage ramp experiments

Pipette solution	Bath solution	V_{rev} (mV)	P_X/P_{K^+}	n
100 mM KCl	100 mM KCl	-0.68 ± 2.71		16
	20 mM KCl	$+35.03 \pm 2.85$	0.0685 (X; Cl^-)	7
100 mM K^+	symmetric	-0.13 ± 1.53		12
(standard solution)	100 mM Li^+	-0.45 ± 2.32	1.02 (X; Li^+)	12
	100 mM Na^+	-2.11 ± 3.04	1.09 (X; Na^+)	8
	100 mM Rb^+	-0.10 ± 3.15	1.00 (X; Rb^+)	8
	100 mM Cs^+	$+1.84 \pm 3.01$	0.93 (X; Cs^+)	8

All ion permeability ratios for large conductance channel were obtained by the voltage ramp experiments. With obtaining the permeability ratios of various monovalent cations, currents carried by anions were neglected, because P_{Cl^-}/P_{K^+} was found to be low.

nels seemed to become saturated. Fig. 5 shows that the channel activities (NP_o) at various Ca^{2+} concentrations that were normalized to those at 10^{-4} M Ca^{2+} for individual patches; they are plotted in the figure against Ca^{2+} concentrations. The best fitting the data revealed a dissociation constant (K_d) of $10^{-5.48}$ M ($= 3.31$ μM) for Ca^{2+} and a Hill coefficient (n) of 4.9. Since the normalized channel activity was more than 1 at 10^{-5} M Ca^{2+}, a large Hill coefficient value was obtained; if the normalized channel activity was 1 at 10^{-5} M Ca^{2+}, a suitable Hill coefficient value might be approximately 3. The curve with $n = 1$ is shown in Fig. 5, demonstrating that the experimental data clearly deviated from the curve with a Hill coefficient of 1. This result suggested that there were more than two Ca^{2+} binding sites should be occupied for full channel activation.

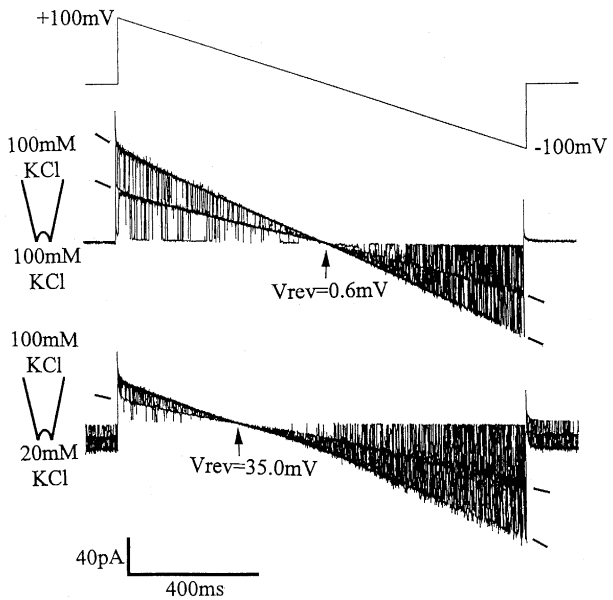

Fig. 2. Ramp experiments for the determination of ion selectivity. Top trace: A wave form of the voltage ramp. Middle trace: Representative current when the patch membrane was applied to the voltage ramp in the symmetrical 100 mM KCl condition. The crossing point of currents marks the reversal potential. This value was estimated by eye, using cursors of the pCLAMP program (*clampfit*). When the bath solution was exchanged to 20 mM KCl, the reversal potential was shifted (bottom trace). These traces were obtained from the same patch membrane; the patch contained two large conductance channels. Each trace (middle and bottom) was repeated with the voltage ramp ten times, and the obtained current traces were superimposed.

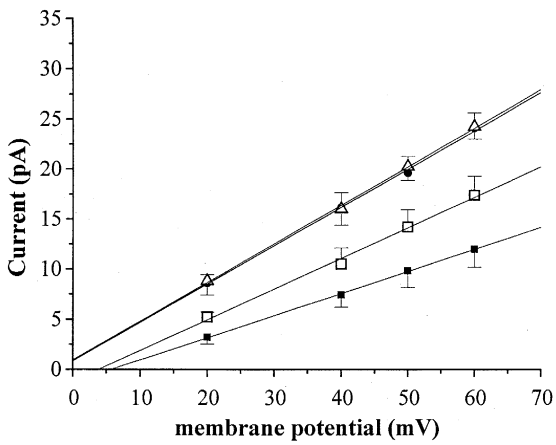

Fig. 3. Current–voltage relationships of the non-selective cation channel for various monovalent cations on the intracellular side. The pipette contained 100 mM K^+ standard solution and the bath contained various cations, 100 mM Rb^+, Na^+, Cs^+ or Li^+ instead of 100 mM K^+. Conductances were estimated by linear regression analysis. Open triangles, filled circles, open squares, filled squares indicate single channel currents for 100 mM Rb^+, Na^+, Cs^+ and Li^+, respectively, in the bath solution.

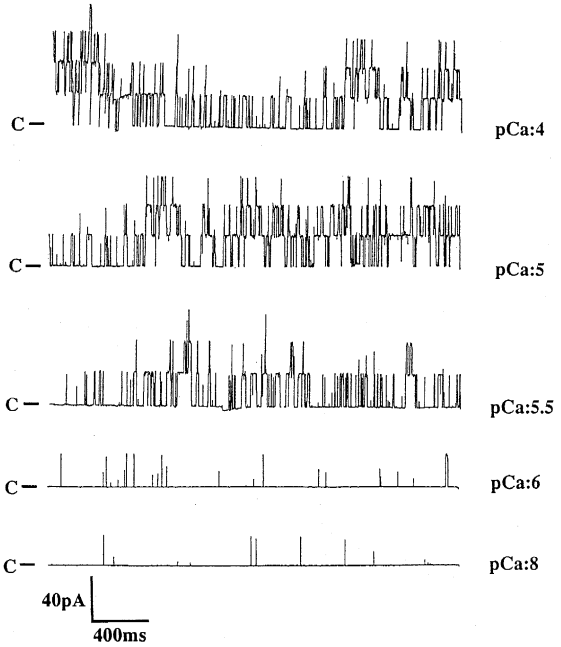

Fig. 4. Single channel activity in 100 mM K^+ standard solution with five different Ca^{2+} concentrations. Little activity was observed at 10^{-8} and 10^{-6} M Ca^{2+} solutions (two bottom traces). The channel was active with above 3.2 μM ($=10^{-5.5}$ M) Ca^{2+} solution. The membrane potential was held at +50 mV. In this case, the patch contained four non-selective cation channels. The intracellular side of the patch was exposed to different Ca^{2+} concentration solutions for approximately 5 s, and then it was washed out with 10^{-8} M Ca^{2+} solution.

3.3. Voltage dependency of channel activity

The channels activated by high Ca^{2+} (>3.2 μM) were more active upon depolarization than hyperpolarization (Fig. 1A). After the activity became stable at 10^{-5} M Ca^{2+}, we examined the voltage dependency of the channel with a series of voltage pulses from −60 to +60 mV for about 20 s each. The channel activity expressed as NP_o was calculated and normalized to the maximal NP_o within a set of data from each patch. The normalized channel activity was plotted against the membrane potential (Fig. 6). An increase in the channel activity was observed upon depolarization. The rate of increase was steep. In contrast, upon hyperpolarization, the normalized channel activity was low and almost no change was observed.

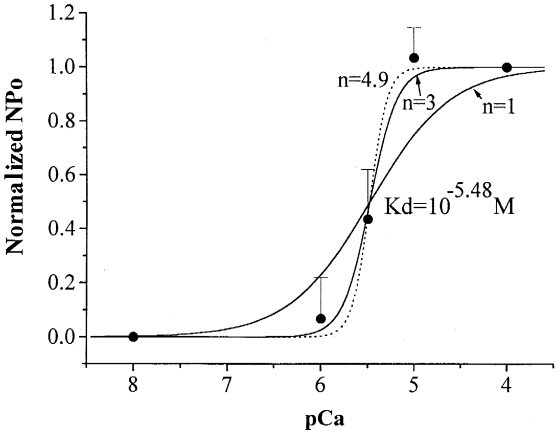

Fig. 5. Ca^{2+} dependency of the channel activity averaged for 5 s from six patches. The channel activities given as NP_o at various Ca^{2+} concentrations were obtained and normalized to that at 10^{-4} M Ca^{2+} for each patch. Finally, normalized NP_o values from six patches were averaged and plotted. These points (mean ± S.D.) were fitted with a sigmoidal curve with the equation: normalized $NP_o = c^n/(c^n + c_o^n)$, where $n = 4.9$; $c_o = 10^{-5.48}$ M; and c is the Ca^{2+} concentration in molar (dotted line). A curve calculated for $n = 1$ and 3 with the same dissociation constant are also drawn for comparison.

3.4. Effects of channel blockers

Various channel blockers are commonly used to classify channel types and to probe the channel architecture. We examined the effects of the K^+ channel

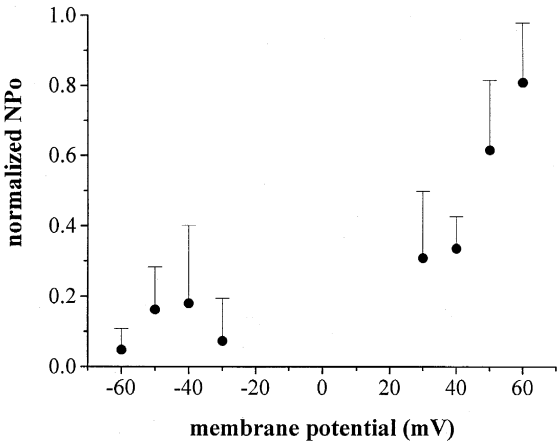

Fig. 6. Voltage dependency of channel activity. The channel activity as NP_o at 10^{-5} M Ca^{2+} was calculated from approximately 12-s segments of current traces upon voltage steps to various levels. NP_o was normalized to the maximum within the set of data from one patch. Normalized NP_o values from six patches were averaged and plotted (mean ± S.D.).

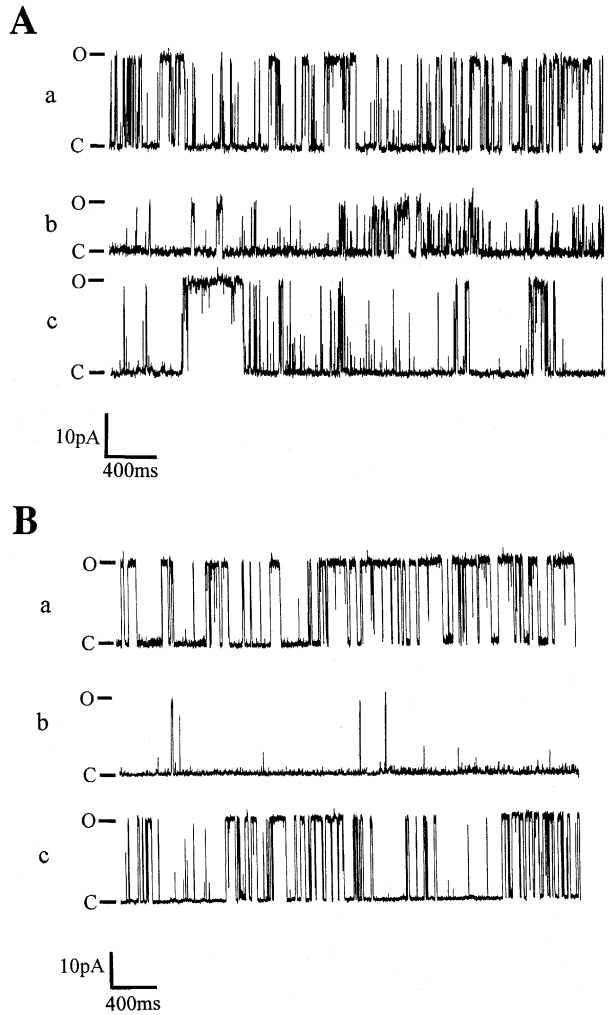

Fig. 7. Effects of K^+ channel blockers. The membrane potential was held at +50 mV, and the concentration of Ca^{2+} in the bath was 10^{-5} M. 'C' and 'O' indicate the closed and open level, respectively. (A) Effect of 10 mM TEA. (B) Effect of 1 mM Ba^{2+}. (a) Before blocker application. (b) After blocker application. TEA reduced the current amplitude, and Ba^{2+} reduced the open probability. (c) After wash-out of the blocker. The effects of both blockers were reversible.

blockers tetraethylammonium (TEA) and Ba^{2+} at the cytoplasmic side. Fig. 7A shows the blockage of the channel by 10 mM TEA. The TEA reduced the current amplitude by 51.9% ($n = 8$). This effect was reversible. Fig. 7B shows the blocking effect of Ba^{2+}; 1 mM Ba^{2+} reduced the channel open probability without reducing the current amplitude. This blocking effect was also reversible.

4. Discussion

Paramecium caudatum (K115) is a mutant cell which was originally selected as a high-K^+ solution resistant type cell. We attempted to record the single channel current by using a wild-type (G3) cell prior to this investigation. In experiments with the wild type, Ca^{2+}-activated K^+ channels which had conductance of about 70 pS were encountered in more than 50% of the patches. We suspected that this channel was the same as the Ca^{2+}-dependent K^+ channel activated upon hyperpolarization reported by Saimi et al. [4]. We also observed the large conductance, Ca^{2+}-dependent cation channel reported here in the wild type, but it was very rare. Contrary to this, although the mutant cells also possessed the 70 pS channel, the large conductance Ca^{2+}-dependent cation channel was observed more often in the mutant type rather than in the wild type.

4.1. Large conductance Ca^{2+}-dependent channel: a non-selective cation channel

The large conductance, Ca^{2+}-dependent cation channel in *Paramecium* reported here is novel. The single channel conductance of the channel was approximately 460 pS (Fig. 1). Although many types of channels have been identified in *Paramecium* cells and reviewed [1,2], only the Cl^- channel had such a large conductance ($\sim$ 430 pS). In the present voltage ramp experiments (Fig. 2), we found that the permeability ratio (P_{Cl^-}/P_{K^+}) of the channel was 0.0685, implying that the channel was more permeable to K^+ than to Cl^-. This channel did not distinguish between K^+ and several monovalent cations (Table 1). Thus, the channel may be described as a non-selective cation channel with poor discrimination of alkali metal ions. Many non-selective cation channels have recently been observed in various cells [9–12,14,15]. However, such channels have small conductances (30–150 pS in $\sim$ 140 mM K^+ or Na^+), and thus differ from the channel described here. Cation channels that were permeable to K^+ and Na^+ were observed in *Paramecium* cell [16]. The channel was activated by ATP and had small channel conductance (150 pS), and thus differs from the channel described here.

This non-selective cation channel was activated by increasing the intracellular Ca^{2+} concentration (Fig. 4). In *Paramecium* cells, some Ca^{2+}-activated channels have been investigated at the single channel level [4–6]. Comparing the properties of those channels, the Ca^{2+} dependency is possibly similar to the Ca^{2+}-calmodulin activated Na^+ channel [6] (Hill coefficient: 4.1 and 3.6, in the absence and in the presence of Mg^{2+}, respectively). However, this Na^+ channel selectively passed Na^+ and not K^+ [6].

In the present study, since the channel activity at pCa = 5 was higher than that at pCa = 4, the Hill coefficient was large (Fig. 5). A suitable value of the Hill coefficient might be approximately 3. This channel was activated upon depolarization (Figs. 1A, 2 and 6). Upon the depolarization of the membrane potential, the channel activity increased steeply. Although we tried to fit the voltage dependency with a Boltzmann distribution, it did not agree with the activities on the hyperpolarization side.

4.2. Single channel conductances with various permeant cations

The large conductance channel showed lack of selectivity for five monovalent cations (Table 1). At negative membrane potentials, the amplitudes of single channel currents were not dependent on the cation present in the bath (data not shown). At positive membrane potentials, the amplitudes of the single channel currents were dependent on the cation present in the bath, and the following conductance sequence for the large conductance non-selective channel was obtained.

$$g_K > g_{Rb} = g_{Na} > g_{Cs} > g_{Li}$$

On a simple one-binding site model, the reversal potential is dependent on the height of the energy barriers, and the conductance depends on both the energy barrier and well depth [17]. Since the reversal potentials of the large conductance non-selective cation channel in different cations were not changed, the barriers were almost the same for all five ions. In contrast, the conductance was dependent on the tested cations, and the one-binding site model predicts that the main difference between these ions comes from the depth of the well. This suggested that only the well depth of the binding site in the channel changed, and increased following the sequence: $K^+ < Rb^+ = Na^+ < Cs^+ < Li^+$.

4.3. Effects of blockers

The K^+ channel blockers, TEA and Ba^{2+}, blocked the Ca^{2+}-activated non-selective cation channels. TEA reduced the value of the single channel currents upon depolarization, and Ba^{2+} reduced the open channel probability upon depolarization. However, the voltage dependency of the blocking effect was not clear since the channel activity was suppressed upon hyperpolarization.

4.4. Comparison with the channel of wild-type cells

The large conductance channels were encountered in more than 30% of the patches from the mutant (K115) cells examined, but in only 7.0% of the patches (6 of 86) from wild-type cells. The ratio of the two types of Ca^{2+}-dependent cation channels might be different in wild-type and the mutant *Paramecium* cells. This difference might cause the high-K^+ solution resistance of the mutant. It may be explained as follows. When *Paramecium* cells were exposed in high-K^+ solution, the membrane potential was depolarized, and then the voltage-dependent Ca^{2+} channels opened. The voltage-dependent Ca^{2+} channels caused Ca^{2+} influx, and the increase of an intracellular Ca^{2+} concentration activated the Ca^{2+}-dependent K^+ channels. This channel caused repolarization. Since this channel was activated upon hyperpolarization, the membrane potential was continuously hyperpolarized by this channel until the intracellular Ca^{2+} concentration decreased. Finally, the leaking of internal K^+ caused cellular death. However, for the mutant cell, when the membrane potential was depolarized by opening of the voltage-dependent Ca^{2+} channel and the Ca^{2+} influx was induced, the non-selective cation channel was activated and caused membrane repolarization. When the membrane potential returned to the resting level, the non-selective cation channel closed and stopped the excess leaking of internal K^+. If the mutant has mainly the non-selective cation channels instead of 70 pS channels as Ca^{2+}-dependent cation channels, the leaking of internal K^+ will become small.

We recently found that the mutant (K115) cells had smaller tail currents induced by hyperpolarization than those of the wild-type cells (unpublished data). We suspect that these currents were caused by the Ca^{2+}-dependent K^+ channels activated by hyperpolarization. The mutant cells may have a small number of the Ca^{2+}-dependent K^+ channels activated by hyperpolarization. Since the wild-type cells also possess this large conductance non-selective channel, further functional studies of this channel remain to be carried out.

References

[1] Y. Saimi, B. Martinac, R.R. Preston, X.-L. Zhou, S. Sukharev, P. Blount, C. Kung, in: D.M. Fambrough (Ed.), Molecular Evolution of Physiological Processes, Rockefeller University Press, New York, 1994, pp. 179–195.
[2] B. Martinac, X.-L. Zhou, A. Kubalski, S. Sukarev, C. Kung, in: C. Peracchia (Ed.), Handbook of Membrane Channels: Molecular and Cellular Physiology, Academic Press, New York, 1994, pp. 447–459.
[3] B.E. Ehrlich, A. Finkelstein, M. Forte, C. Kung, Science 225 (1984) 427–428.
[4] Y. Saimi, B. Martinac, J. Membr. Biol. 112 (1989) 79–89.
[5] X.-L. Zhou, C.W.M. Chan, Y. Saimi, C. Kung, J. Membr. Biol. 144 (1995) 199–208.
[6] Y. Saimi, K.-L. Ling, Science 249 (1990) 1441–1444.
[7] F. Saitow, Y. Nakaoka, Photochem. Photobiol. 63 (1996) 868–873.
[8] D. Colquhoun, E. Neher, H. Reuter, C.F. Stevens, Nature 294 (1981) 752–754.
[9] S.A. Lipton, Biochim. Biophys. Acta 856 (1986) 59–67.
[10] N.C. Sturgess, C.N. Hales, M.L.J. Ashford, FEBS Lett. 208 (1986) 397–400.
[11] V. von Tscharner, B. Prod'hom, M. Baggiolini, H. Reuter, Nature 324 (1986) 369–372.
[12] R. Sabovcik, J. Li, P. Kucera, B. Prod'hom, J. Gen. Physiol. 106 (1995) 149–174.
[13] I.I. Pottosin, FEBS Lett. 308 (1992) 87–90.
[14] H. Chang, S. Ciani, Y. Kidokoro, J. Physiol. 476 (1994) 1–16.
[15] K. Minami, K. Fukuzawa, I. Inoue, Pflügers Arch. 426 (1994) 254–257.
[16] Y. Saimi, B. Martinac, A.H. Delcour, P.V. Minorsky, M.C. Gustin, M.R. Culbertson, J. Adler, C. Kung, in: B. Rudy, L.E. Iverson (Eds.), Methods in Enzymology, vol. 207, Academic Press, New York, 1992, pp. 681–691.
[17] B. Hille, Ionic Channels of Excitable membranes, 2nd ed., Sinauer, MA, 1992.